GW190814: Gravitational Waves from the Coalescence of a 23 Solar Mass Black Hole with a 2.6 Solar Mass Compact Object

Jan 20, Team C

Ay215

A brief history of LIGO observations

Sept 12, 2015
LIGO O1 Begins
Livingston +
Hanford
~80 Mpc

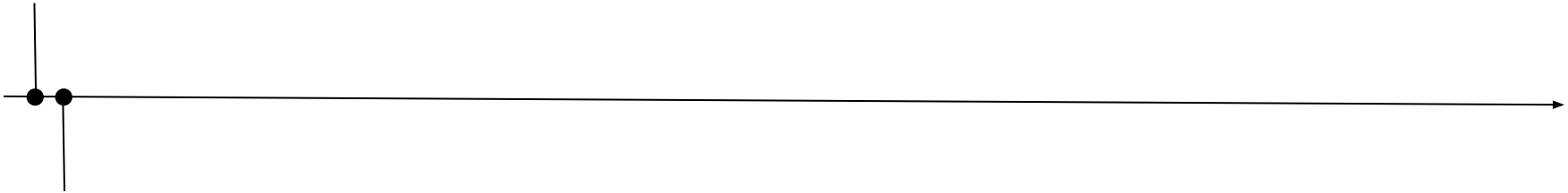

Sept 14, 2015
GW150914
Luminosity dist: 410 Mpc
BH Masses: 36+29 Msun

* Sensitivities quantified by BNS range, average distance a BNS merger can be observed

A brief history of LIGO observations

Sept 12, 2015
LIGO O1 Begins
Livingston +
Hanford
~80 Mpc

Nov 30, 2016
LIGO O2 Begins
Livingston +
Hanford
~100 Mpc

Aug 17, 2017
GW170817
Luminosity dist: 40 Mpc
Total Mass: 2.74 Msun

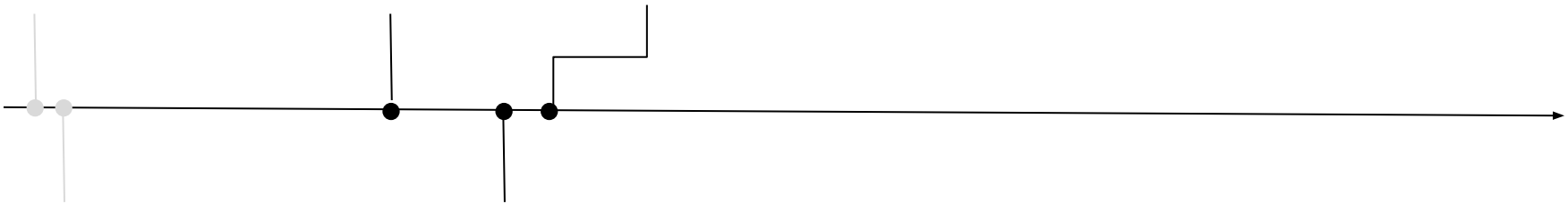

Sept 14, 2015
GW150914
Luminosity dist: 410 Mpc
BH Masses: 36+29 Msun

Aug 1, 2017
Advanced Virgo
comes online
~30 Mpc

* Sensitivities quantified by BNS range, average distance a BNS merger can be observed

A brief history of LIGO observations

Sept 12, 2015
LIGO O1 Begins
Livingston + Hanford
~80 Mpc

Sept 14, 2015
GW150914
Luminosity dist: 410 Mpc
BH Masses: 36+29 Msun

Nov 30, 2016
LIGO O2 Begins
Livingston + Hanford
~100 Mpc

Aug 1, 2017
Advanced Virgo comes online
~30 Mpc

Aug 17, 2017
GW170817
Luminosity dist: 40 Mpc
Total Mass: 2.74 Msun

Apr 1, 2019
LIGO/Virgo O3 Begins
Livingston: 125-140 Mpc
Hanford: 102-111 Mpc
Virgo: 43-50 Mpc

Aug 14, 2019
GW190814
Luminosity dist: 241 Mpc
BH Mass: 22.2 - 24.3 Msun
Companion: 2.5 - 2.67 Msun

* Sensitivities quantified by BNS range, average distance a BNS merger can be observed

Matched Filtering Search Algorithms

Chirp Mass

$$M = \frac{(m_1 m_2)^{3/5}}{(m_1 + m_2)^{1/5}}$$

Symmetric Mass Ratio

$$\eta = \frac{m_1 m_2}{(m_1 + m_2)^2}$$

Spin Parameters

$$\chi = \frac{cS}{Gm^2}$$

Matched Filtering Search Algorithms

GstLAL

- Time-dependent waveform template matching
- Used for real time event identification

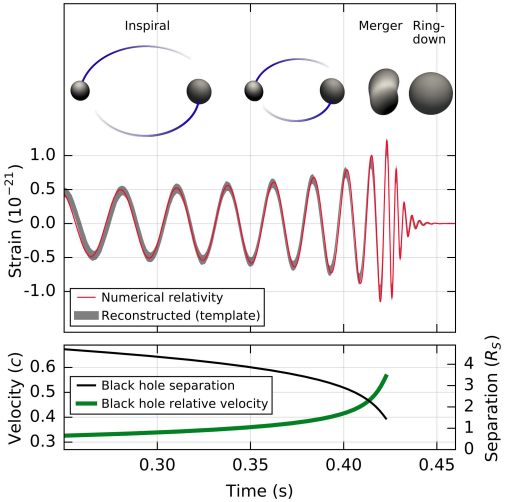

PyCBC

- Generate templates using power spectrum density

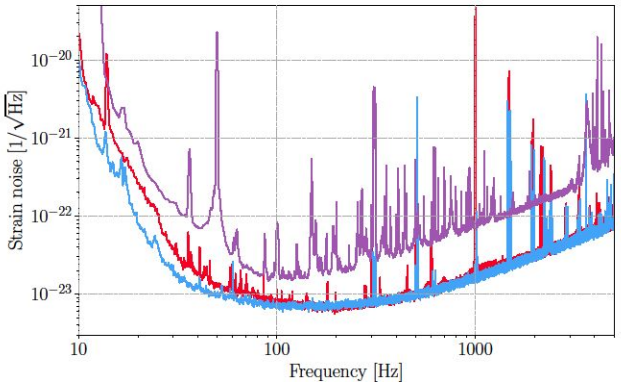

Detection and Localization of GW190814

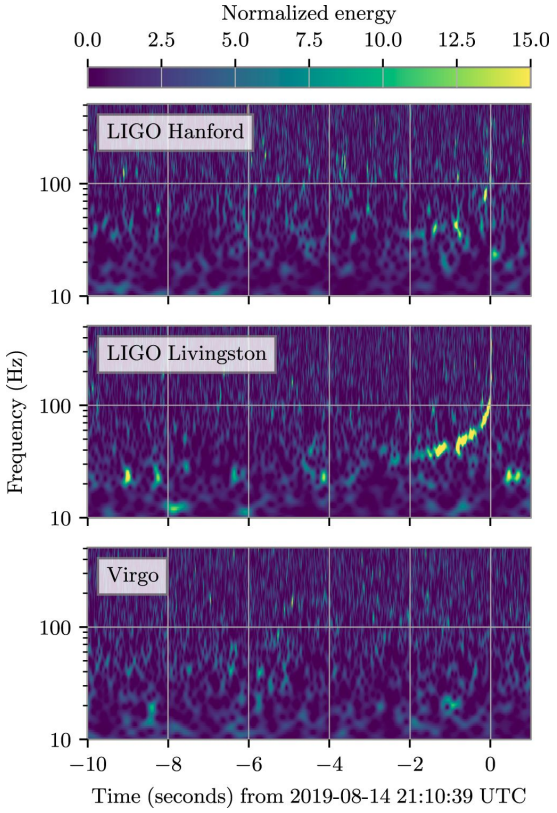

	Initial Identification with GstLAL	Verification with PyCBC
LIGO Hanford		SNR: 10.6
LIGO Livingston	SNR: 21.4	SNR: 21.6
Virgo	SNR: 4.3	SNR: 4.5
	Classification: MassGap	Classification: NSBH

Localization of GW190814

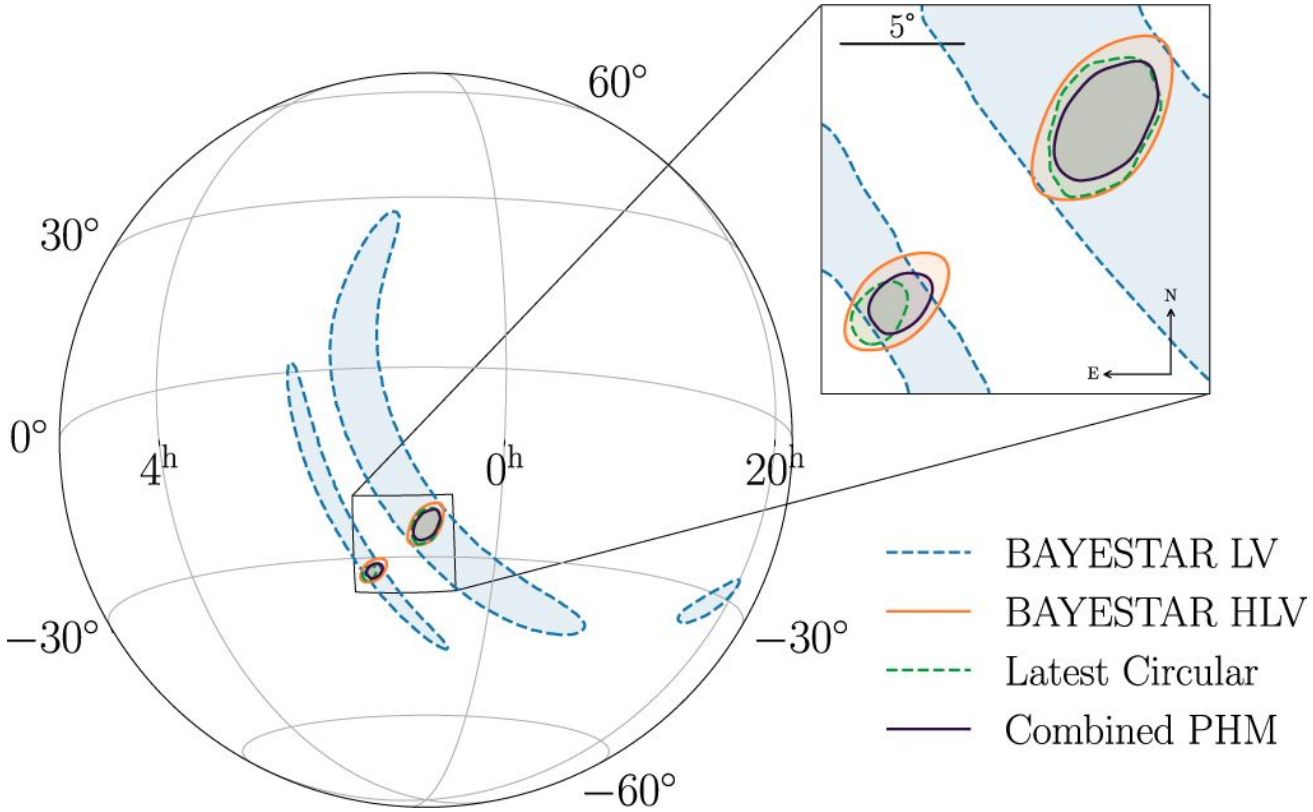

Multimessenger Follow-up

Merger Type	EM Counterpart Expected?
Binary Black Hole	No
Binary Neutron Star	Yes
Black Hole + Neutron Star	Yes for low mass ratio (M_BH <= ~9M_sun) Otherwise no

Significance Estimate

False Alarm Rate (FAR)

Conservative Estimate

GstLAL: 1 in 1300 yr PyCBC: 1 in 8.1 yr

Including estimation of noise distribution

GstLAL: 1 in 10^5 yr PyCBC: 1 in 4 x 10^4 yr

Physical parameters of a BBH binary

- Kerr black hole only defined by mass and spin, for a BBH 8 intrinsic parameters: m_1, m_2, $\mathbf{S}_1$, $\mathbf{S}_2$, + 7 extrinsic parameters:
  - Sky location (α,δ)
  - Luminosity distance d_L
  - Orbital inclination and polarization angle
  - Time and phase at coalescence
  -
- Maximum spin for a Kerr BH: Gm^2/c ->
  - dimensionless spin vector $\boldsymbol{\chi}_i = c\mathbf{S}_i / (Gm_i^2)$
  - dimensionless spin magnitude $a_i = cS_i / (Gm_i^2)$
- If spins have a component in the orbital plane, then they precess along the total angular momentum $\mathbf{J} = \mathbf{L} + \mathbf{S}_1 + \mathbf{S}_2$. Dominant spin effects are described introducing effective parameters.

Physical parameters of a BBH binary

- Effective aligned spin:

$$\chi_{eff} = \frac{\left(m_1 \vec{\chi}_1 + m_2 \vec{\chi}_2 \right) \cdot \hat{L}_N}{\left(m_1 + m_2 \right)}$$

Positive (negative) values of χ_{eff} increase (decrease) the number of orbits from any given separation to merger (degenerate with q). Approximately conserved during inspiral

- The phase evolution depends on leading order on the chirp mass

$$\mathcal{M} = \frac{\left(m_1 m_2 \right)^{3/2}}{\left(m_1 + m_2 \right)^{1/5}}$$

- The mass ratio $q = m_2/m_1$ and χ_{eff} appear at higher orders (harder to constrain)
- Effective precession spin:

$$\chi_p = max\left[\frac{\left\| \vec{S}_{1\perp} \right\|}{m_1^2}, \kappa \frac{\left\| \vec{S}_{2\perp} \right\|}{m_2^2} \right], \qquad \kappa = q \frac{(4q+3)}{(3+4q)}$$

For a binary containing a NS

- Additional degrees of freedom related to the NS response to a tidal field. The dominant quadrupole (l=2) tidal deformation is described by the dimensionless tidal deformability:

$$\Lambda = \frac{2}{3} k_2 \left(\frac{c^2 R}{Gm} \right)^5$$

, where k_2 is the dimensionless l=2 Love number

Analysis to determine physical properties

- Bayesian inference: $$p(\vec{\theta}|\vec{d}) = \frac{p(\vec{d}|\vec{\theta})\,p(\vec{\theta})}{p(\vec{d})}$$

- $\vec{\theta}$: vector of parameters for the model -> hypothesis
- $\vec{d}$: observed data
- $p(\vec{\theta}|\vec{d})$:posterior -> probability of the hypothesis given the observation
- $p(\vec{\theta})$: prior -> probability of the hypothesis before the observation. In the paper most parameters are given a uniform prior
- $p(\vec{d}|\vec{\theta})$: likelihood -> compatibility of observation with given hypothesis. In the paper: combination between detector response and a parametrized waveform model for the GW polarizations to obtain the strain.
- Also, as the masses are redshifted, they assume a standard ΛCDM cosmology to calculate the redshift from the distance.

Analysis to determine physical properties

- Waveforms used in the paper:
  - for BBH: EOBNR (effective one body approach) and Phenom (phenomenological approach)
  - for NSBH: same as for BBH but augmented with tidal effects

From the NSBH waveform they obtain a posterior on Λ_2 uninformative relative to a uniform prior, so no measurable tidal deformability.

This is consistent with BBH but also with NSBH because of the low mass ratio: the binary merges before NS is tidally disrupted (independently of EOS)

Properties

Table 1

Source Properties of GW190814: We Report the Median Values Along with the Symmetric 90% Credible Intervals for the SEOBNRV4PHM (EOBNR PHM) and IMRPHENOMPV3HM (PHENOM PHM) Waveform Models

	EOBNR PHM	Phenom PHM	Combined
Primary mass $m_1/M_\odot$	$23.2^{+1.0}_{-0.9}$	$23.2^{+1.3}_{-1.1}$	$23.2^{+1.1}_{-1.0}$
Secondary mass $m_2/M_\odot$	$2.59^{+0.08}_{-0.08}$	$2.58^{+0.09}_{-0.10}$	$2.59^{+0.08}_{-0.09}$
Mass ratio q	$0.112^{+0.008}_{-0.008}$	$0.111^{+0.009}_{-0.010}$	$0.112^{+0.008}_{-0.009}$
Chirp mass $\mathcal{M}/M_\odot$	$6.10^{+0.06}_{-0.05}$	$6.08^{+0.06}_{-0.05}$	$6.09^{+0.06}_{-0.06}$
Total mass $M/M_\odot$	$25.8^{+0.9}_{-0.8}$	$25.8^{+1.2}_{-1.0}$	$25.8^{+1.0}_{-0.9}$
Final mass $M_f/M_\odot$	$25.6^{+1.0}_{-0.8}$	$25.5^{+1.2}_{-1.0}$	$25.6^{+1.1}_{-0.9}$
Upper bound on primary spin magnitude χ_1	0.06	0.08	0.07
Effective inspiral spin parameter $\chi_{\rm eff}$	$0.001^{+0.059}_{-0.056}$	$-0.005^{+0.061}_{-0.065}$	$-0.002^{+0.060}_{-0.061}$
Upper bound on effective precession parameter χ_p	0.07	0.07	0.07
Final spin χ_f	$0.28^{+0.02}_{-0.02}$	$0.28^{+0.02}_{-0.03}$	$0.28^{+0.02}_{-0.02}$
Luminosity distance D_L/Mpc	235^{+40}_{-45}	249^{+39}_{-43}	241^{+41}_{-45}
Source redshift z	$0.051^{+0.008}_{-0.009}$	$0.054^{+0.008}_{-0.009}$	$0.053^{+0.009}_{-0.010}$
Inclination angle Θ/rad	$0.9^{+0.3}_{-0.2}$	$0.8^{+0.2}_{-0.2}$	$0.8^{+0.3}_{-0.2}$
Signal-to-noise ratio in LIGO Hanford ρ_H	$10.6^{+0.1}_{-0.1}$	$10.7^{+0.1}_{-0.2}$	$10.7^{+0.1}_{-0.2}$
Signal-to-noise ratio in LIGO Livingston ρ_L	$22.21^{+0.09}_{-0.15}$	$22.16^{+0.09}_{-0.17}$	$22.18^{+0.10}_{-0.17}$
Signal-to-noise ratio in Virgo ρ_V	$4.3^{+0.2}_{-0.5}$	$4.1^{+0.2}_{-0.6}$	$4.2^{+0.2}_{-0.6}$
Network Signal-to-noise ratio ρ_{HLV}	$25.0^{+0.1}_{-0.2}$	$24.9^{+0.1}_{-0.2}$	$25.0^{+0.1}_{-0.2}$

Spins

- Tight constrains on χ_{eff} thanks to long inspiral
- χ_p is hard to measure for face-on or face-off, but since inclination ~0.8 rad -> strong constraints on χ_p as well. Strongest constraint for a GW event

Strong constraints on χ_p also help constraining the secondary mass:

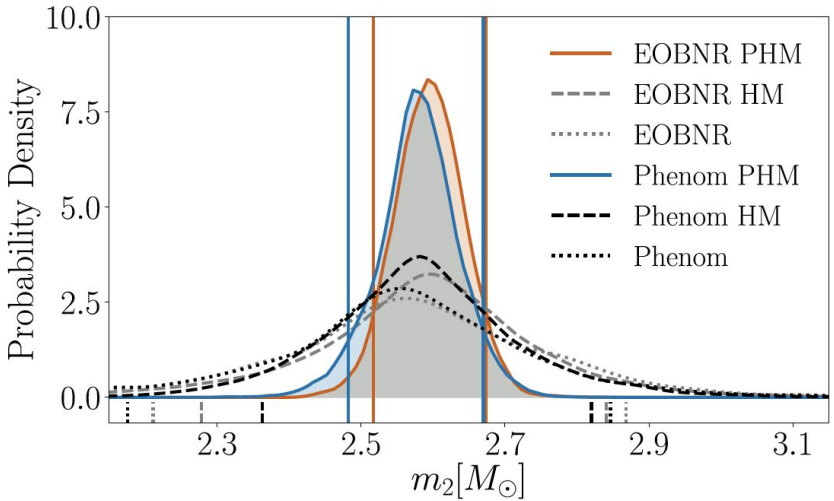

Spins

- The more massive object dominates contribution to χ_p and χ_p -> strongest constraints for primary spin

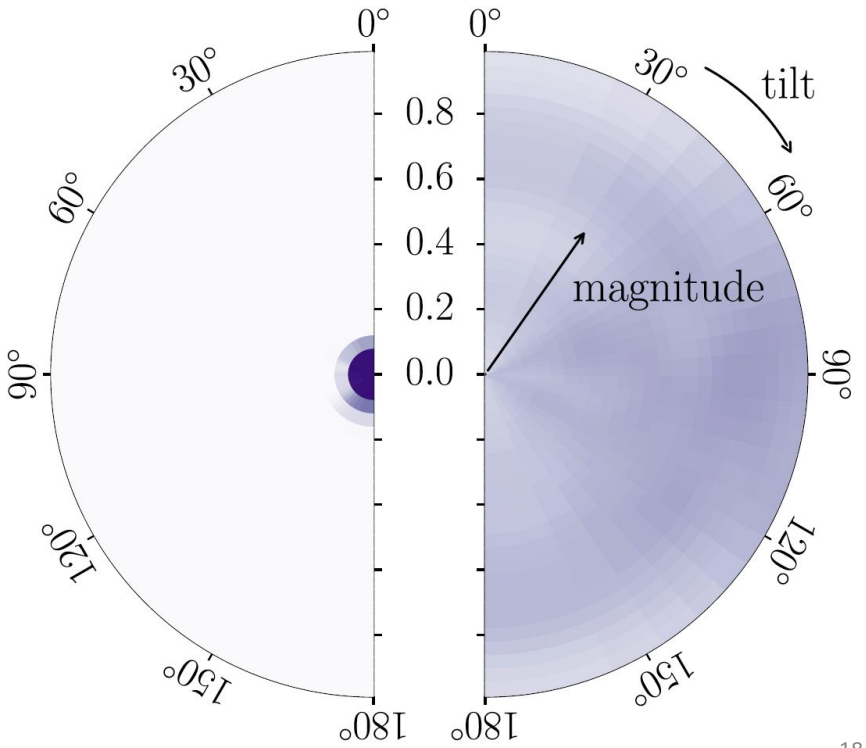

Evidence for Higher-order Multipoles

- Comparing models with the Bayes' number: $\log_{10}\mathcal{B} \simeq 9.6$ in favor of model with higher multipole moments vs only (2,2)

Evidence for Higher-order Multipoles

- Comparing models with the Bayes' number: $\log_{10}\mathcal{B} \simeq 9.6$ in favor of model with higher multipole moments vs only (2,2)
- Comparing strongest subdominant multipole S/N with Gaussian noise

Each multipole is decomposed into parts parallel and perpendicular to the dominant multipole by calculating the overlap between it and the dominant multipole.

Orthogonal S/N of (l,m)=(3,3) in orange

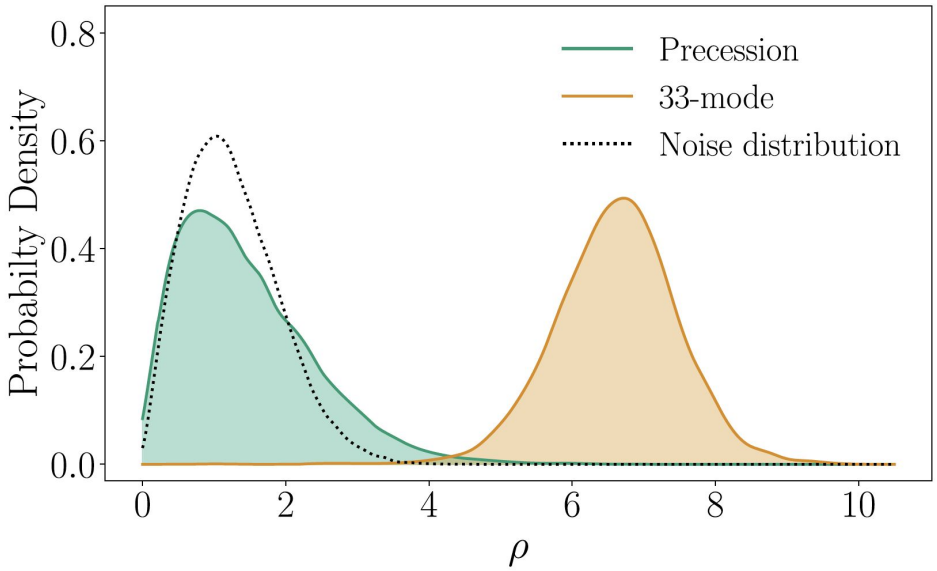

Evidence for Higher-order Multipoles

- Comparing models with the Bayes' number: $\log_{10}\mathcal{B} \simeq 9.6$ in favor of model with higher multipole moments vs only (2,2)
- Comparing strongest subdominant multipole S/N with Gaussian noise
- Check the presence of higher multipoles in the time-frequency signal

$$f_{lm}(t) \simeq \frac{m}{2} f_{22}(t) \equiv \alpha f_{22}(t)$$

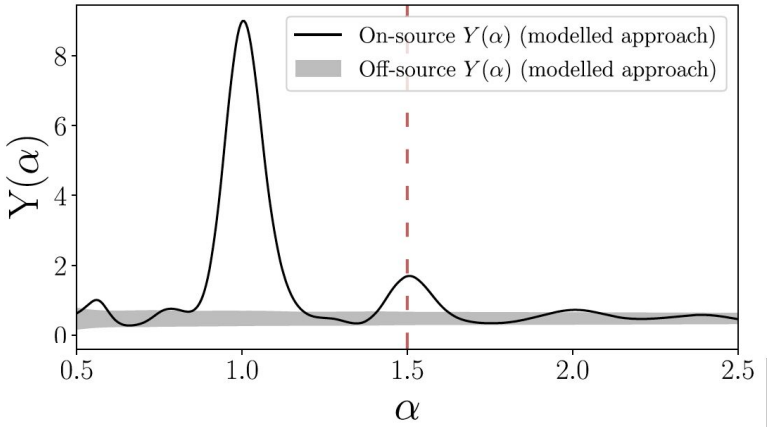

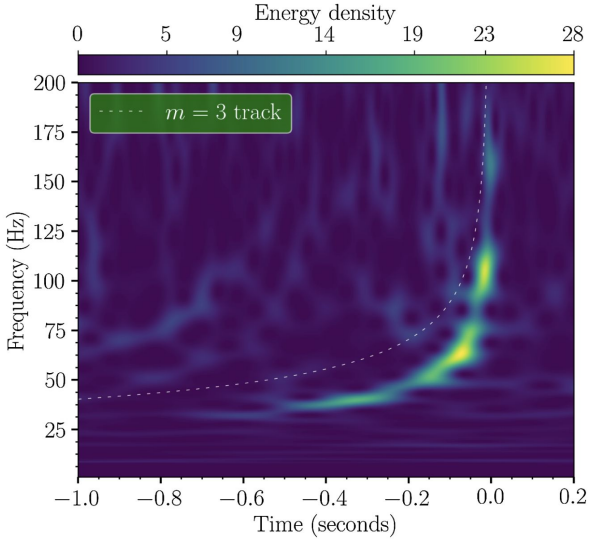

Evidence for Higher-order Multipoles

- Comparing models with the Bayes' number: $\log_{10}\mathcal{B} \simeq 9.6$ in favor of model with higher multipole moments vs only (2,2)
- Comparing strongest subdominant multipole S/N with Gaussian noise
- Check the presence of higher multipoles in the time-frequency signal

Additional method: reconstruct signal using waveform-agnostic methods and compare with predictions from a waveform model without higher multipoles:

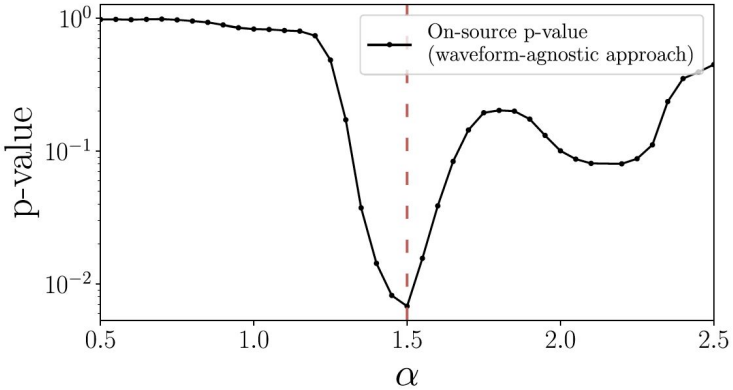

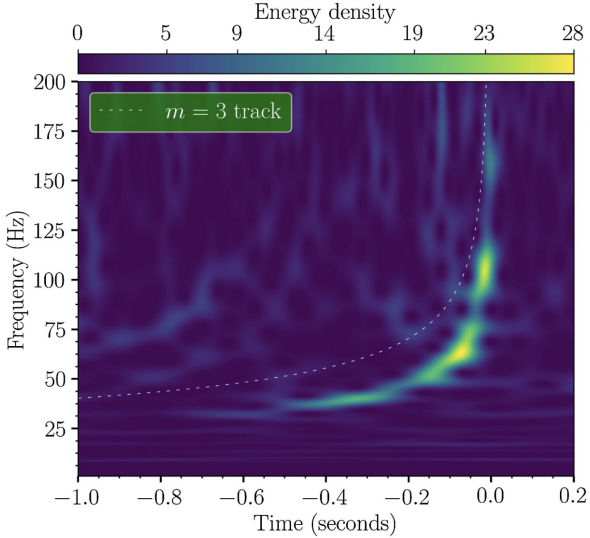

Tests of GR

- New region of parameter space: very unequal mass ratio. Also, higher multipoles signal can put stronger constraints on deviations from GR.
- Method: looking for inconsistencies between the observed signal and predictions of GR

- 1: they subtract the maximum likelihood waveform from the data and look at **residuals** -> consistent with noise
- 2: look at deviations in the **spin-induced quadrupole moment κ** (κ=1 for BH, κ=2-14 for NS), but they cannot constrain it because with small χ_{eff} bounds are weak
- 3: parametrized test of gravitational waveform generation with **post-Newtonian coefficients**. They find no deviation from GR predictions.

Merger rate density

Take GW190814 as a new class of compact binary merger “GW190814-like event”

$$\mathcal{R} = \frac{N_{\rm obs}}{\langle VT \rangle}$$

Tiwari 2018

$\langle VT \rangle$: surveyed spacetime volume

- product of sensitive volume $\langle V \rangle$ and time T during which $N_{\rm obs}$ observations have been made
- Calculate $\langle VT \rangle$ semi-analytically with imposed S/N threshold 5 (single) / 10 (network)
- calibrated to match results from pipelines assuming once-per-century FAR threshold

Merger rate density

- search pipeline sensitivity is estimated by simulated signals with source properties uniformly distributed in
  - comoving volume
  - component masses : 2.5 - 40 M_{sun} for BH, 1 - 3 M_{sun} for NS
  - component spins (aligned with orbital L) : < 0.95

- injected waveform models : Phenom PHM / EOBNR PHM

- for GW190814-like systems, $\mathcal{R} = 7^{+16}_{-6}\,\mathrm{Gpc}^{-3}\mathrm{yr}^{-1}$

cf) BBH merger rate from GWTC-2 : $\mathcal{R}_{\mathrm{BBH}} = 23.9^{+14.9}_{-8.6}\,\mathrm{Gpc}^{-3}\,\mathrm{yr}^{-1}$

LIGO Scientific and Virgo Collaborations, 2020

Secondary object - NS? BH?

m_2 = 2.6 M_{sun} falls in mass gap (2.5 - 5 M_{sun})

compare m_2 with $M_{\max}$ (maximum non-rotating NS mass estimate)

<u>inference by reconstructed EOS</u>

$m_2 \leq M_{\max}$ ~ 3%

<u>NS mass measurements</u>

$M_{\max} = 2.25^{+0.81}_{-0.26}\, M_\odot$

$m_2 \leq M_{\max}$ ~ 30%

<u>Constraint by GW170817</u>

Absolute upper bound $\sim 2.7 M_\odot$

$M_{\max} \sim 2.2 - 2.3 M_\odot$

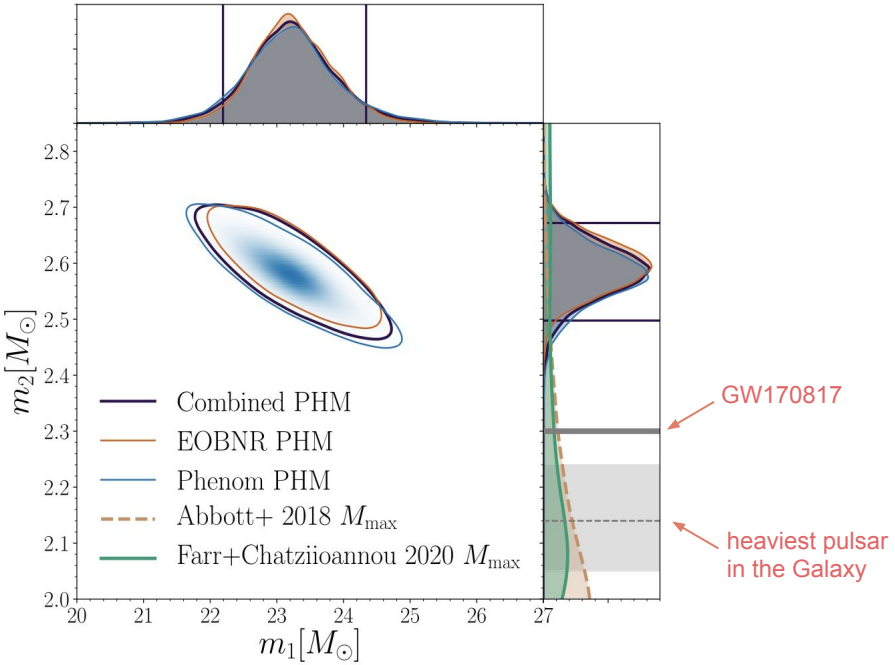

Fig 3 from paper

Secondary object - NS? BH?

- Overall, GW190814 secondary seems not to be NS.
  However..
  - Secondary spin is unconstrained -- can be rapidly rotating enough to exceed $M_{\max}$
    Still, unlikely to maintain extreme NS spin before merge
  - exotic compact object?

- What if secondary is NS? (potential implications for neutron star EOSs)

favors stiffer EOSs

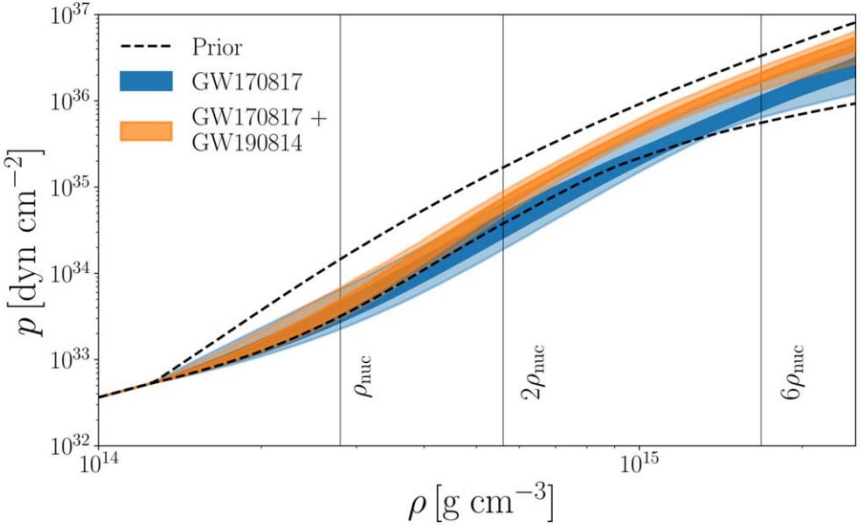

Fig 8 from paper

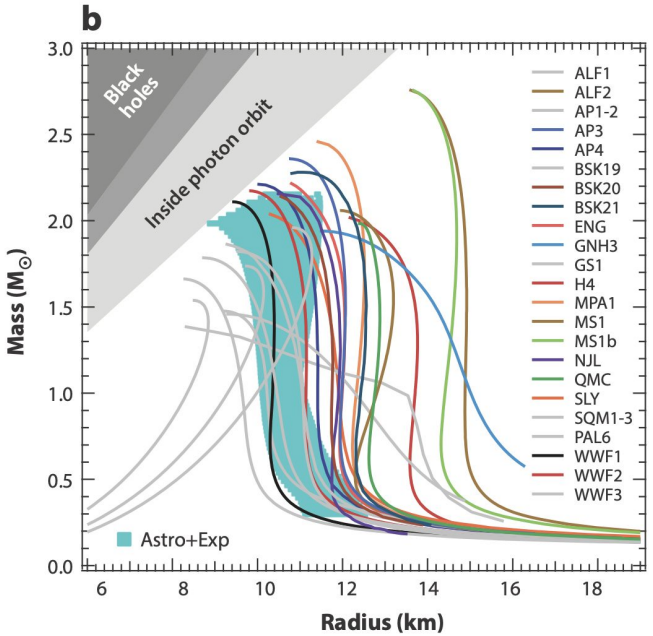

Özel & Freire 2016

- What if secondary is NS? (potential implications for neutron star EOSs)

favors stiffer EOSs

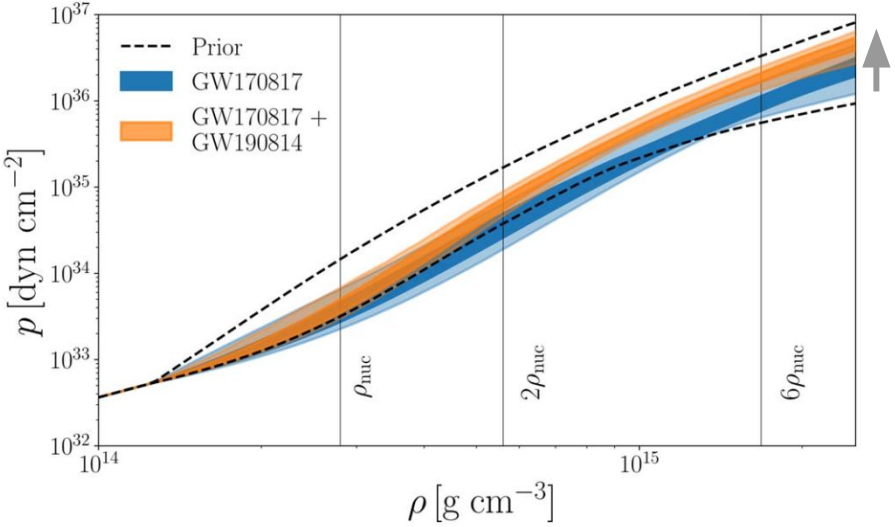

Fig 8 from paper

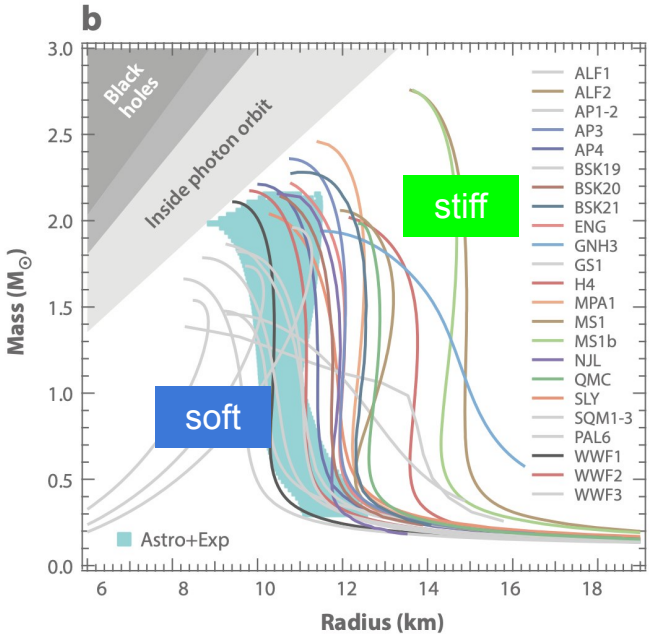

Özel & Freire 2016

Origin of GW190814-like systems

mass gap + unequal mass + inferred rate
(q=0.112)

Compact star formation models

- robust discovery of an object within mass gap

Population synthesis models

- most BBH mergers : $q > 0.5$
- NSBH binaries : very rare $q \lesssim 0.1$
- tend to disfavor unequal masses

Dynamical origin (stellar clusters)

- most BBH mergers $q \sim 1$
- NSBH formation suppressed
- young clusters : promising hosts for GW190814-like events

Hierarchical triple/quadruple

Disk around SMBHs in AGN

- challenging to explain, but potentially consistent with multiple formation scenarios

Cosmological implications

Luminosity distance (from GW)
+
source redshift (from EM)

→ constrain cosmological parameters

*most sensitive to LIGO-Virgo : H_0

- EM counterparts (e.g. GW170817)
- cross-correlation of GW localization
- neutron star EOS
- GW mass + distribution

GW190814 $H_0 = 75^{+59}_{-13}\ \mathrm{km\ s^{-1}\ Mpc^{-1}}$

GW190814 + GW170817 $H_0 = 70^{+17}_{-8}\ \mathrm{km\ s^{-1}\ Mpc^{-1}}$

Conclusion

- On Aug 14 2019, LIGO-Virgo observed GW190814
  - a novel source unlike any other compact binary mergers, shedding new light on compact object mass distribution.

- Secondary can be (i) the lightest BH, or (ii) the heaviest NS discovered in compact binary systems.
  - NS scenario is unlikely, but cannot be firmly excluded

- Unique properties of this event poses a challenge for our understanding of the population of merging compact binaries